Soft Matter

Accepted Manuscript

Volume 12 | Number 1 | 7 January 2016 | Pages 1–314

Soft Matter

www.softmatter.org

ISSN 1744-683X

ROYAL SOCIETY OF CHEMISTRY

PAPER
Jure Dobnikar et al.
Rational design of molecularly imprinted polymers

175 YEARS

ROYAL SOCIETY OF CHEMISTRY

Journal Name

ARTICLE

Unravelling the 2D Self-Assembly of Fmoc-Dipeptides at Fluid Interfaces

Pablo G. Argudo,[a] Rafael Contreras-Montoya,[b] Luis Álvarez de Cienfuegos,[*b] Juan M. Cuerva,[b] Manuel Cano,[a] David Alba-Molina,[a] María T. Martín-Romero,[a] Luis Camacho,[a] Juan J. Giner-Casares*[a]

Dipeptides self-assemble onto supramolecular structures showing plenty of applications in nanotechnology and biomedical fields. A set of Fmoc-dipeptides with different aminoacid sequences has been synthesized and their self-assembly at fluid interfaces has been assessed. The relevant molecular parameters for achieving an efficient 2D self-assembly process have been established. The self-assembled nanostructures of Fmoc-dipeptides displayed significant chirality and retained the chemical functionality of the aminoacids. The impact of the sequence in the final supramolecular structure has been evaluated in high detail using *in situ* characterization techniques at air/water interface. This study provides a general route for the 2D self-assembly of Fmoc-dipeptides.

Introduction

Dipeptides are an exciting building block in nanotechnology.[1–8] Dipeptides display some advantageous features among self-assembling organic molecules, such as easy choice in sequence during synthesis, readily available chiral features and high biocompatibility, with Fmoc-dipeptides as highly promising structure, especially in biological applications.[9] Intracellular NO delivery was achieved by a purposefully self-assembling dipeptide.[10] Fmoc (9-fluorenylmethyloxycarbonyl) group contributes to enhance the self-assembly of the dipeptides onto well-defined nanostructures through solvophobic interactions, also providing amphiphilic character.[11–13] Self-assembly of Fmoc-dipeptides in bulk solution is able to render nanowires with excellent chirality and energy transfer features.[14,15] Intriguingly, self-assembled nanowires of dipeptides are connected to the core recognition motif in Alzheimer disease.[16] Supramolecular structures of dipeptides are also promising candidates as antibacterial agents for membrane disruption, alternatively to standard antibiotics that promote acquired bacterial resistance.[17] The amphiphilic

character of the Fmoc-dipeptides leads to interesting applications as ultrathin membranes for local control of physicochemical parameters.[18] Remarkably, the local value of pH is crucial for the efficient self-assembly of the dipeptides.[19] Moreover, the Fmoc-dipeptides are highly interesting in technological applications based in self-assembled nanostructures by purposefully designed building blocks.[20] Stable emulsions can be fabricated using Fmoc-dipeptides as stabilizing surfactants at the oil/water interface, with the possibility of tuning the emulsion properties by simply varying the sequence of the dipeptide. The self-assembly process at the oil/water interface is also promoted by other similar groups to Fmoc, *e. g.*, Pyrene, however Fmoc yields optimum results.[21,22] The self-assembly capability of a given dipeptide sequence might determine the actual performance in applications as in vivo self-assembly for biomedical purposes.[23,24]

A large body of research is devoted to the self-assembly of dipeptides to render functional and interesting nanostructures. Orientation on the influence of the aminoacid sequence in the self-assembly process that might guide a purposefully chemical synthesis is highly desirable.[25] Nevertheless much of the published work has been restricted to the isotropic growth in bulk solution mediated by a self-assembly process triggered by different stimuli, such as pH, solvent, temperature or enzymatic.[26] The influence of many experimental factors makes very difficult to predict the gel-forming capacity of specific sequences of aminoacids in bulk solution, although recent works have tried to achieve this goal using a combination of sophisticated computational and true data analysis within families of peptides.[27,28] On the contrary, a systematic study involving the self-assembly of small peptides in 2D and connecting the aminoacid sequence with the

a. *Departamento de Química Física y T. Aplicada, Instituto Universitario de Investigación en Química Fina y Nanoquímica IUIQFN, Facultad de Ciencias, Universidad de Córdoba, Campus de Rabanales, Ed. Marie Curie, E-14071 Córdoba, Spain. E-mail: jjginer@uco.es*
b. *Departamento de Química Orgánica, Facultad de Ciencias, Universidad de Granada, (UGR), C. U. Fuentenueva, Granada E-18071, Spain. E-mail: lac@ugr.es*
Electronic Supplementary Information (ESI) available: Experimental details, Figures S1-S15: solid phase synthesis protocol and ^1H and ^{13}C-NMR spectra copies of Fmoc-CF, Fmoc-MF and Fmoc-RF, surface pressure-molecular area isotherms, UV-vis reflection spectra, Brewster angle microscopy pictures, DLS measurements, circular dichroism spectra, assessment of the UV-vis bands of the Fmoc group and the Fmoc-dipeptides in bulk solution, Molecular Dynamics Simulations of self-assembled Fmoc-FF at the air/water interface, application of the Extended Dipole Model for assessment of the UV-vis reflection spectra. DOI: 10.1039/x0xx00000x

ARTICLE

achieved nanostructure has never been carried out. The possibility to create functional surfaces simply by coating with small peptides brings many new applications in bio- and nanotechnology, such as biologically active surfaces that can interact with cells, antimicrobial, superhydrophobic, optical or chiroptical surfaces.[29,30]

Here we present a framework for the 2D self-assembly of Fmoc-dipeptides at fluid interfaces. Relevant molecular parameters are defined in terms of aminoacid sequence and experimentally tested. The supramolecular structures were successfully built from the 2D self-assembly of the Fmoc-dipeptides at the air/water interface and studied in detail by utilizing the Langmuir technique. The air/water interface provides a rather experimentally simple and reliable route for the 2D self-assembly of the Fmoc-dipeptides.[31] Note that in all cases we use Fmoc-derived dipeptides herein, thus taking advantage of the amphiphilic character promoted by the self-assembling Fmoc group. The experimental techniques for characterization included herein assured the in situ measure of the nanostructures exclusively placed at the air/water interface, with no contribution from bulk solution. In addition to provide a comprehensive model for 2D self-assembly of dipeptides at fluid interfaces, detailed information on the molecular arrangement of the dipeptide units at the interface is shown.[32] Guiding rules for the chemical design of Fmoc-dipeptides that efficiently self-assemble at fluid interfaces are provided by relating the aminoacid sequence of the Fmoc-dipeptides with the self-assembling capabilities.

Results and discussion

A set of Fmoc-dipeptides was synthesized, see Scheme 1, section SI1. Two Fmoc-aminoacids were included as well for further confirming the range of application of the molecular parameters defined in our model, Fmoc-Y (Tyrosine) and Fmoc-F (Phenylalanine). A carboxyl group was included as end group in all cases to assure the sole dependence of the nanostructures on the aminoacid sequence.[33] The aqueous subphase was in all cases a diluted HCl solution (pH = 2) to enhance the self-assembly of the Fmoc-dipeptides on the air/water interface.[34] The Fmoc-dipeptides were not located at the air/water interface when using Milli-Q water with almost neutral pH, see SI6. The following dipeptides were able to self-assemble at the air/water interface: Fmoc-CF (Cysteine-Phenylalanine), Fmoc-MF (Methionine-Phenylalanine), and Fmoc-FF (diphenylalanine). On the other hand, the following dipeptides were not anchored at the air/water interface, instead being solved in the bulk water solution: Fmoc-LG (Leucine-Glycine), Fmoc-AA (dialanine), Fmoc-GG (diglycine), and Fmoc-RF (Arginine- Phenylalanine), see Figures SI2,3. The presence of the not self-assembling dipeptides at the air/water interface was ruled out according to the absence of UV-vis spectroscopy signal and any observable microstructure, see SI4,5. The layers of Fmoc-dipeptides were compressed at a speed of 0.03 nm^2 min^{-1} molecule^{-1}, typically considered in

Langmuir studies as a speed value suitable for studying equilibrium structures. Unfortunately, the surface active Fmoc-dipeptides were transferred into the water subphase after compression. Therefore, experiments dealing the kinetics of assembly of the Fmoc-dipeptides could not be performed.

Scheme 1. Molecular structure of the Fmoc-dipeptides.
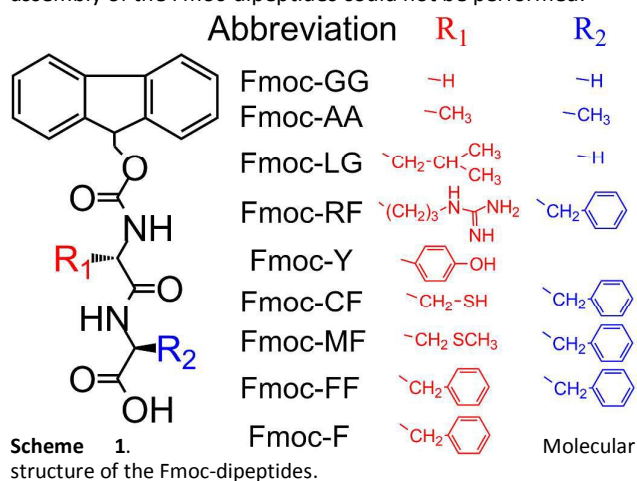
Note all the Fmoc-dipeptides displayed a certain amphiphilic character provided by the hydrophobic and self-stacking Fmoc group and a markedly polar headgroup, *i. e.*, the carboxylic acid. Intriguingly, such amphiphilicity does not guarantee the interfacial self-assembly of all the Fmoc-dipeptides. This finding was in agreement with the report on Fmoc-dipeptides as stabilizing agents for oil/water emulsions by Ulijn *et al.*, who found that the aminoacid sequence strongly determines the residence of the Fmoc-dipeptides at the oil/water interface. The chemical modification of the sequence of the Fmoc-dipeptides could then lead to an enhanced stability of the oil/water emulsions based on Fmoc-dipeptides.[21] Herein we offer insights on the 2D behavior of Fmoc-dipeptides at the air/water interface that can be extended to the formulation of oil/water emulsions stabilized by Fmoc-dipeptides. Inspired by the work by Adams and Frith, the partition coefficient *P* and water solubility *S* as relevant and easily calculated molecular parameters were obtained for all Fmoc-dipeptides.[35] The Chemicalize/ChemAxon platform was used for performing the calculations.[36] The log *P* tool calculates the octanol/water partition coefficient, based on the work by Viswanadhan *et al.* and modified according to Klopman.[37,38] The log *S* tool uses a fragment-based method that identifies different structural fragments in the molecule and calculates their relative contribution to the solubility coefficient.[39] Note the log *P* and – log *S* values of the Fmoc-RF indicate a comparatively higher solubility of Fmoc-RF in water than expected from the partition coefficient. The greater solubility of Fmoc-RF is ascribed to the Arginine residue, displaying a larger number of sites for H-bond formation with water.

Journal Name ARTICLE

Two regimes of self-assembling capabilities of Fmoc-dipeptides were obtained, see Figure 1. The Fmoc-dipeptides tended to be solved in bulk solution rather than self-assemble at the air/water interface for low values of log P and $-$log S (high hydrophilicity). The soluble Fmoc-dipeptides formed aggregates in bulk water, as confirmed by dynamic light scattering measurements, see SI7.[40] Oppositely, those Fmoc-dipeptides with high values of log P and $-$log S were able to self-assemble into well-defined supramolecular structures at the air/water interface (high hydrophobicity). The range of values for the partition coefficient of the tested Fmoc-dipeptides extended *ca.* five orders of magnitude.
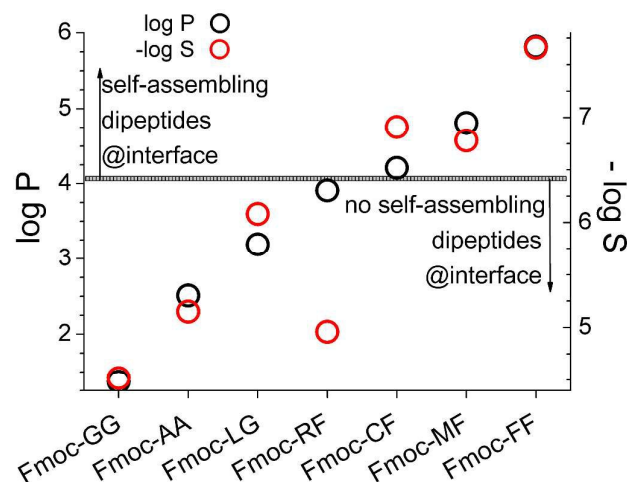

Figure 1. Values of log P (black circles) and log S (red circles) for the Fmoc-dipeptides. Two regimes can be differentiated: Zone of no self-assembling dipeptides for log P and $-$log S lower than 4.1 and 6.4, respectively; Zone of self-assembling dipeptides for log P and $-$log S higher than 4.1 and 6.4, respectively. A transition zone is indicated as a dividing box.

A transition zone at log P of *ca.* 4.1 and $-$log S of *ca.* 6.4 was found as the limit between the two regimes. This limit might serve as an indication when chemically designing dipeptide derivatives for stabilizing oil/water emulsions. The Fmoc-dipeptides were chosen to fully cover a representative range of values of solubility and partition coefficient. Whereas these findings might not be applied to all derivatives of Fmoc-dipeptides, this criterion is valid for our set of Fmoc-dipeptides and provides a semiquantitative approximation for the chemical design of dipeptides for 2D self-assembly.

This criterion for defining the efficient 2D interfacial self-assembly is exclusive for the Fmoc-dipeptides. Fmoc-Y and Fmoc-F display log P = 4.4 and 4.7 and $-$log S = 5.5 and 5.9, respectively. Fmoc-F was able to self-assemble at the air/water interface, as opposed to Fmoc-Y, thus probing their distinct behaviour with respect to the Fmoc-dipeptides.

Brewster Angle Microscopy (BAM) is an optical technique that allowed direct visualization solely of the microstructures formed by the Fmoc-dipeptides in situ at the air/water interface. No contribution from bulk solution was recorded in the BAM pictures. The presence of the Fmoc-dipeptides induced the change of refractive index of the air/water interface and therefore the visualization of the microstructures was achieved. Figure 2 and SI8-11 shows the BAM pictures of the Fmoc-dipeptides acquired at the air/water interface. Well-defined elongated ribbon-like microstructures were observed for Fmoc-MF and Fmoc-FF, arising from stacking and lateral packing of the Fmoc-dipeptide molecules. The thickness of the microstructures was 2.6±0.8 and 2.4±0.6 μm for the Fmoc-MF and Fmoc-FF dipeptides, respectively. A modest influence of the sequence on the final morphology of the microstructures was observed.

Electron microscopy measurements confirmed the thickness value of the supramolecular structure, with a thickness of 1.0±0.5 μm, see below. 2D self-assembly led to larger assemblies than those obtained by 3D assembly in bulk solution, typically with a thickness from *ca.* 20 to 200 nm.[40,41] Note the thickness values were obtained by measuring the image with the ImageJ software, and therefore these values might be taken only as a semiquantitative approach. The apparent discrepancy between the two values of thickness was ascribed to the different conditions for measuring, *e. g.*, the electron microscopy picture was taken under high vacuum and extremely low content of water, whereas the BAM pictures were taken in contact with the water surface in laboratory conditions. Therefore, the lower value of thickness for the nanostructures under vacuum conditions was expected due to the drying of the sample.

Remarkably, decrease of the available surface area was able to reduce the distance between the microstructures formed by the Fmoc-dipeptides with no significant modification of the thickness. Further compression induced packing of the microstructures onto a continuous solid film as observed by BAM, see SI8-11. The temperature was kept constant at 21 ºC, given the significant influence of temperature on the Fmoc-dipeptide nanostructures.[42]
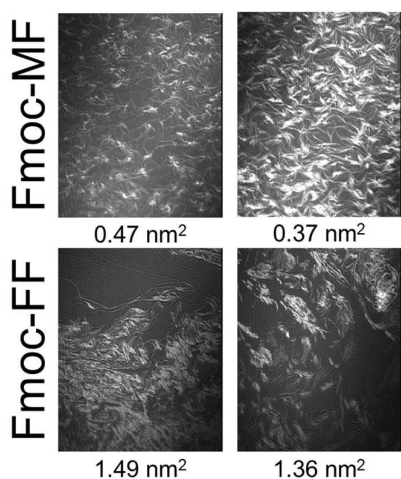
Figure 2. Brewster Angle Microscopy (BAM) pictures at the air/water interface of Fmoc-MF and Fmoc-FF (top and bottom pictures, respectively). The value of available surface area per molecule of Fmoc-dipeptide is included at the bottom of each picture. The width of each frame corresponds to 215 μm.

The Fmoc-dipeptides self-assembled at the air/water interface display chirality. The supramolecular structures formed by Fmoc-dipeptides could be readily transferred to a solid support by gently touching the air/water interface with a solid support, *i. e.*, using the Langmuir-Schaeffer technique. The fidelity of the transfer process Fmoc-dipeptides onto solid substrates was checked by comparing the UV-vis spectra obtained by transmission (solid substrates) and reflection (air/liquid interface) UV-vis spectroscopy. The shape and relative intensity of the band remains constant after the transference, see Figure SI12. We therefore assume that the perturbation induced by the transfer of the layers of Fmoc-dipeptides is not significant.

A significant circular dichroism (CD) signal related to the supramolecular organization of the Fmoc group into highly ordered self-assembled structures was obtained, see Figure 3, SI13,14. Both chiral centers for all the Fmoc-dipeptides included in this study were (S,S). Two positive bands for Fmoc-MF and Fmoc-FF at ca. 212 nm and 264 nm was related to n→π* and π→π* transitions of the Fmoc group, respectively. These two bands indicated a similar self-assembly to related Fmoc-dipeptides.[43] This arrangement was confirmed by the band at *ca.* 194 nm from the Fmoc-FF supramolecular structures, typically arising from the interaction of the π-π* transition of the amide I band with the aromatic rings of the dipeptides.[44] The positive sign of all CD bands indicated a unique supramolecular organization of the Fmoc-FF obtained
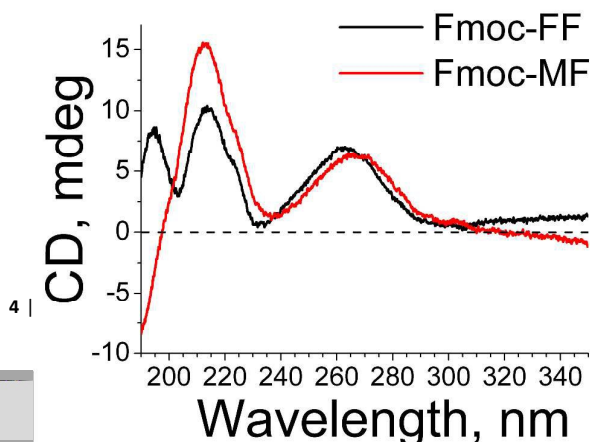
using this 2D self-assembly route, probably imposed by the arrested organization at the air/water interface in contrast to 3D bulk formation of hydrogels with negative signals in CD, see SI14.[45,46]

Figure 3. Circular dichroism spectra of the 2D self-assembled Fmoc-FF (black line, 15 layers transferred), Fmoc-MF (red line, 10 layers transferred) transferred to a quartz support by the Langmuir-Schaeffer technique.

Quantitative information on the presence and orientation of the Fmoc groups at the air/water interface could be conveniently obtained by in situ UV–vis reflection spectroscopy. The signal was recorded exclusively at the air/water interface, based on the increase of reflection of incoming radiation from the presence of the Fmoc-dipeptide molecules at the interface according to eq. (1):

$$\Delta R_{norm} = A \times \Delta R = \frac{2.303 \times 10^{17} f_0 \varepsilon}{N_A} \sqrt{R_S} = 5.41 \times 10^{-8} f_0 \varepsilon \tag{1}$$

where ΔR_{norm} has $nm^2 \cdot molec^{-1}$ units, R_S is the air/water interface reflectivity, A and ε are the available surface area and the absorption coefficient per Fmoc-dipeptide molecule, respectively.[47] f_0 is the orientation factor, accounting for a preferential orientation of the transition dipole of the Fmoc group at the self-assembled supramolecular structures. The value of f_0 was experimentally obtained from the UV-vis reflection spectra. Limit values of f_0 = 1.5 and 0 are defined, indicating that the transition dipole of Fmoc is either parallel or perpendicular to the water surface, respectively, see SI15. This is the first study providing quantitative insights on the molecular arrangement of the Fmoc-dipeptides at fluid interfaces.

Figure 4 shows the 2D UV-vis reflection spectra as well as the 3D bulk transmission spectra for the Fmoc-FF dipeptide. A shift to longer wavelength of *ca.* 4 nm was obtained when comparing the UV-vis reflection spectra with the bulk spectrum. This shift corresponds to the formation of J-aggregates and local changes in polarizability in the self-assembled supramolecular structure formed by the Fmoc-FF dipeptide. The shape of the band centred at 265 nm of the Fmoc-FF 2D supramolecular structures was slightly modified when compared to the non-assembled Fmoc-FF in bulk solution. The bulk spectrum of Fmoc-FF in bulk solution was formed by four components at a 276, 265, 262, and 255 nm, with the most intense component at 265 nm. The UV-vis reflection spectra of Fmoc-FF at the air/water interface were formed by four components at a 281, 269, 262 and 258 nm, with the most intense component at 262 nm. This change in the shape of the UV-vis band was ascribed to the change of orientation of the polarization axes of the Fmoc group at the air/water interface. The Fmoc-FF molecules might display a preferential orientation at the interface that differs from bulk due to the restricted geometry of the 2D interface, as further confirmed by the CD results, see above. The relative

ARTICLE

orientation of the Fmoc group of the Fmoc-FF dipeptide at the air/water interface was assessed from the UV-vis reflection spectra. An orientation factor value of $f_0 = 1.5$ was obtained, indicating a parallel orientation of the longitudinal axis of the Fmoc group to the water surface. No shift in the UV-vis reflection bands is observed at different values of available surface area per Fmoc-FF molecule. Thus, the supramolecular arrangement of the Fmoc group was not modified by the decrease in the surface area of the nanowires, instead being determined by the self-assembly of the Fmoc-dipeptide units.
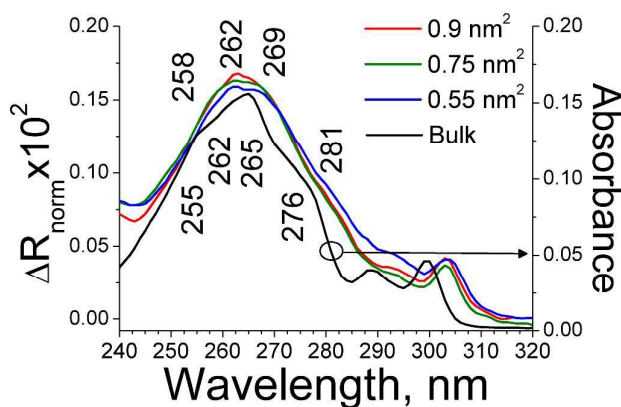

Figure 4. UV-vis reflection (red, green and blue lines indicating different values of available surface area) and bulk solution (black line) spectra for the Fmoc-FF dipeptide. Maximum values of wavelength for each band and available surface area are indicated in the inset.

The aminoacid sequence of the Fmoc-dipeptides showed a significant influence on the supramolecular arrangement at the air/water interface that can be followed by in situ UV-vis reflection spectra, see SI15.1. A shift of *ca.* 4 nm for the 2D reflection spectra compared to the 3D bulk spectrum was obtained for the Fmoc-CF dipeptide, similarly to the Fmoc-FF dipeptide. However, the shape and relative intensity of the bands remained as observed in bulk solution, indicating a fixed parallel orientation of the main axis of the Fmoc group at the interface, see SI15.2. The Fmoc-MF dipeptide showed a reduced UV-vis reflection intensity when compared to the expected values assuming an $f_0 = 1.5$, as well as further reduction with the decrease of the available surface area. A significant change in morphology of the UV-vis reflection spectra was obtained with the decrease of the available surface area, with the band at 301 nm shifting to 303 nm and a significant modification of the group of bands at 265 nm, probably indicating a change of orientation of the Fmoc group, see SI15.3. Fmoc-F showed a greatly reduced intensity of the UV-vis reflection spectra and no modification of the morphology of the bands upon decrease of the available surface area, indicating a diminished residence at the interface, see SI15.4. The residence of the supramolecular structures of the Fmoc-dipeptides at the air/water interface was assessed by monitoring the maximum intensity of the UV-vis reflection band at 263-270 nm upon decrease of the available surface area. Fmoc-FF was the only Fmoc-dipeptide

showing no loss of molecules onto the subphase with the decrease of the available surface area. The residence of the Fmoc-dipeptide molecules varied according to: Fmoc-FF > Fmoc-CF > Fmoc-MF, see Figure SI15.5. Therefore, high values of log *P* and –log *S* led to persistent assemblies at the air/water interface. This trend might be applied for designing oil/water emulsions stabilized by Fmoc-dipeptides and requiring high stability against long storage times. Therefore we conclude that the interfacial self-assembly of the Fmoc-dipeptides was directed by the sequence of each dipeptide and might be tuned by including the adequate residues.

The molecular arrangement of the Fmoc-dipeptide molecules in the self-assembled supramolecular structures was assessed using Fmoc-FF as foremost example. Molecular dynamics (MD) simulations were performed to attain a fine detail in the supramolecular structure, see Figure 5 and section SI16. The relative position of the Fmoc groups obtained by MD is experimentally tested by calculating the shift in the UV-vis spectra of the UV-vis reflection spectra of the 2D self-assembled Fmoc-dipeptides compared to the bulk solution spectrum (λ_N). The extended dipole model was used, see eq. (2) and SI17:

$$\lambda_{i,N} = \frac{\lambda_{mon}hc10^7}{hc10^7 + 4\lambda_{mon}\sum_{j=k}^{N}J_{1,k}\dfrac{(N+1-k)}{N}} \quad (2)$$

λ_{mon} is the maximum wavelength for the Fmoc-FF in bulk solution, N is the number of Fmoc-FF molecules forming the optically active supramolecular unit. $J_{1,k}$ is the interaction energy between the dipoles of the *1* and *k* Fmoc-FF molecules. Remarkably, an excellent agreement between the MD simulation results, predicting a shift of *ca.* 4 nm with the spectroscopic data showing a shift of 4 nm, see above. The Fmoc groups self-assembled in a zipper-like manner on the air/water interface, see Figure 5. The tilting values of the Fmoc groups with respect to the air/water interface were 76.4º and 72.5º for the longitudinal and transversal axis, respectively. The average distance between the rows of Fmoc groups was 3.4 Å and between neighbouring Fmoc was 10.7 Å, see Figure 5. Note that the rows of Fmoc-FF were shifted 2.5 Å upwards with respect to the front row.
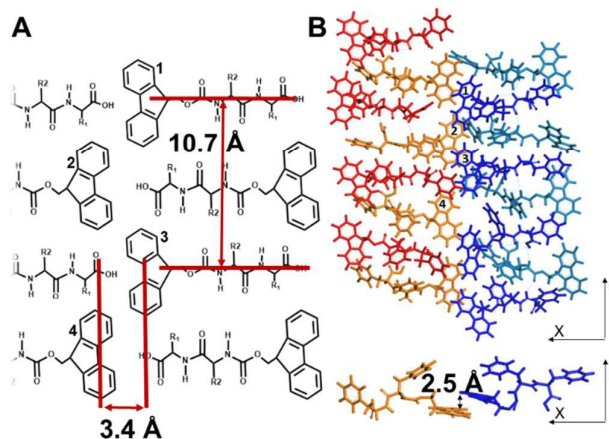
ARTICLE

Journal Name

Figure 5. A) Molecular sketch of the arrangement of the inter-molecular distance of Fmoc groups. B) Caption of molecular dynamics simulations for the Fmoc-FF dipeptide on the XY (interface) and XZ planes. Numbers 1 to 4 are included to guide the correspondence of atoms between the two schemes.

The 2D self-assembly led not only to well-defined supramolecular structures, but also provided a direct route to include additional building blocks, as demonstrated by Banerjee *et al.* in hydrogels based on Fmoc-dipeptides including graphene.[48] Our previous work shows the possibility of combining dipeptides with Fe nanoparticles.[45] The chemical functionality provided by each aminoacid was conveniently maintained in the nanostructures after the 2D self-assembly. The self-assembled Fmoc-dipeptides presented here showed a highly versatile nanostructure that could be combined with inorganic nanoparticles to form composites at the nanoscale.[49–51]

The attachment of Au nanoparticles with a diameter of 94±5 nm to the 2D self-assembled Fmoc-CF was achieved under simple immersion in a solution of Au nanoparticles of the ribbon-like structures transferred to a glass support. The Fmoc-CF was selected for its chemical functionality allowing the covalent binding of Au nanoparticles. The cysteine residue of the Fmoc-CF was used as a chemical linker to the Au nanoparticles via thiol chemistry, see scheme 1.[52] The Au nanoparticles were attached to the surface of the Fmoc-CF supramolecular structures as a dense monolayer, with certain regions showing an additional layer of nanoparticles, see Figure 6. The supramolecular structures of Fmoc-CF showed an average thickness of 1.0±0.5 μm, in agreement with the BAM pictures, see above. The possibility of using the chemical function of the aminoacid residue of the Fmoc-dipeptide even after forming the assemblies is largely appealing. Moreover, this experimental result supports the proposed supramolecular arrangement. Additional chemical functionalities might be included in the Fmoc-dipeptides, allowing the formation of well-defined hybrid nanocomposites.
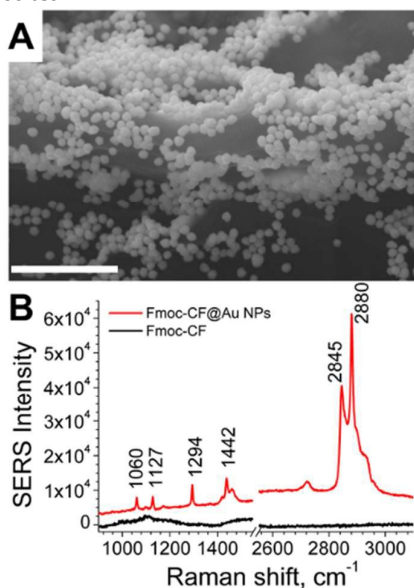
Figure 6. A) Scanning electron microscopy picture of the Fmoc-CF supramolecular structures with attached Au nanoparticles of *ca.* 90 nm diameter. Scale bar is 1 μm. B) SERS performance of the Fmoc-CF supramolecular structures coated by Au nanoparticles. Raman spectrum of self-assembled Fmoc-CF deposited on glass (black line). SERS spectrum of self-assembled Fmoc-CF coated with Au nanoparticles deposited on glass (red line), offset of 5x10^{-3} intensity units.

Surface Enhanced Raman Scattering (SERS) could then be performed due to the close contact of the tightly packed Au nanoparticles with the Fmoc-dipeptides, associated with the formation of "hot-spots".[53,54] The SERS spectrum of the Fmoc-CF is shown in Figure 6B, demonstrating the dramatic enhancement of the Raman signal over the bare Fmoc-CF supramolecular structures. The strong bands at 2845 and 2880 cm^{-1} could be assigned to the symmetric stretch of the $CH_2(CO)$ group and the C–H stretching mode, respectively.[55,56] The bands at 1060 and 1127 cm^{-1} correspond to the asymmetric stretch of the CCO group and the combination of in-plane bending of the CH ring with the bending of CH(H), respectively. The bands at 1294, 1442 cm^{-1} correspond to the in-plane bending of the CH ring, and the bending of the $CH_2(CHCOO)$ terminal group, respectively.[56]

Conclusions

In summary, the first study on 2D self-assembly of Fmoc-dipeptides at the air/water interface onto well-defined supramolecular structures is presented. General guidelines for selecting the amino-acid sequence of Fmoc-dipeptides that will efficiently self-assemble at fluid interfaces have been introduced. By experimentally testing a set of dipeptides with a variety of aminoacid residue sequences, the values of log *P* and -log *S* have been proposed as simple and reliable molecular parameters for deciding whether a given Fmoc-dipeptide would efficiently self-assemble at fluid interfaces. These insights might be extended to the formulation of oil/water emulsions stabilized by Fmoc-dipeptides. The as-obtained supra-molecular structures from the Fmoc-dipeptides retain the chiral features observed in bulk self-assembly. The arrangement of the Fmoc-dipeptide molecules has been convincingly described in high detail by a combination of *in situ* UV-vis spectroscopy and BAM offering information exclusively from the air/water interface. The chirality transfer from the peptides to solid surfaces allows an easy access to chiral surfaces with potential chiroptical applications. The chemical functionality of the Fmoc-dipeptides is maintained after the 2D self-assembly. Moreover, the possibility of forming nanocomposites has been demonstrated by combining a cysteine-containing nanostructure with plasmonic Au nanoparticles, showing SERS effect. This work suggests that Fmoc-dipeptides are relevant bioinspired molecules for self-assembling at fluid interfaces and that the required aminoacid

ARTICLE

sequence for nanostructure design can be efficiently predicted.

Conflicts of interest

There are no conflicts to declare.

Acknowledgements

Notes and references

1   R. Krishna Kumar, R. L. Harniman, A. J. Patil and S. Mann, *Chem. Sci.*, 2016, **7**, 5879–5887.

2   H. Ni, Z. Yu, W. Yao, Y. Lan, N. Ullah and Y. Lu, *Chem. Sci.*, 2017, **8**, 5699–5704.

3   R. Xing, C. Yuan, S. Li, J. Song, J. Li and X. Yan, *Angew. Chem. Int. Ed.*, 2018, **57**, 1537–1542.

4   L. McDougall, E. R. Draper, J. D. Beadle, M. Shipman, P. Raubo, A. G. Jamieson and D. J. Adams, *Chem. Commun.*, 2018, **54**, 1793–1796.

5   B. Sun, H. Riegler, L. Dai, S. Eickelmann, Y. Li, G. Li, Y. Yang, Q. Li, M. Fu, J. Fei and J. Li, *ACS Nano*, 2018, **12**, 1934–1939.

6   G. G. Scott, P. J. McKnight, T. Tuttle and R. V. Ulijn, *Adv. Mater.*, 2016, **28**, 1381–1386.

7   J. Wang, K. Liu, L. Yan, A. Wang, S. Bai and X. Yan, *ACS Nano*, 2016, **10**, 2138–2143.

8   J. Boekhoven, A. M. Brizard, M. C. A. Stuart, L. Florusse, G. Raffy, A. Del Guerzo and J. H. van Esch, *Chem. Sci.*, 2016, **7**, 6021–6031.

9   P. Makam and E. Gazit, *Chem. Soc. Rev.*, 2018, **47**, 3406–3420.

10   H. A. Pal, S. Mohapatra, V. Gupta, S. Ghosh and S. Verma, *Chem. Sci.*, 2017, **8**, 6171–6175.

11   S. Fleming, S. Debnath, P. W. J. M. Frederix, T. Tuttle and R. V. Ulijn, *Chem. Commun.*, 2013, **49**, 10587-10589.

12   S. Murillo-Sánchez, D. Beaufils, J. M. González Mañas, R. Pascal and K. Ruiz-Mirazo, *Chem. Sci.*, 2016, **7**, 3406–3413.

13   A. C. Baumruck, D. Tietze, L. K. Steinacker and A. A. Tietze, *Chem. Sci.*, 2018, **9**, 2365–2375.

14   D. Yang, P. Duan, L. Zhang and M. Liu, *Nat. Commun.*, 2017, **8**, 15727.

15   M. Deng, L. Zhang, Y. Jiang and M. Liu, *Angew. Chem. Int. Ed.*, 2016, **55**, 15062–15066.

16   M. Reches and E. Gazit, *Science*, 2003, **300**, 625–627.

17   L. Schnaider, S. Brahmachari, N. W. Schmidt, B. Mensa, S. Shaham-Niv, D. Bychenko, L. Adler-Abramovich, L. J. W. Shimon, S. Kolusheva, W. F. DeGrado and E. Gazit, *Nat. Commun.*, 2017, **8**, 1365.

18   E. K. Johnson, D. J. Adams and P. J. Cameron, *J. Am. Chem. Soc.*, 2010, **132**, 5130–5136.

19   J. Rodon Fores, M. L. Martinez Mendez, X. Mao, D. Wagner, M. Schmutz, M. Rabineau, P. Lavalle, P. Schaaf, F. Boulmedais and L. Jierry, *Angew. Chem. Int. Ed.*, 2017, **56**, 15984–15988.

20   K. Tao, A. Levin, L. Adler-Abramovich and E. Gazit, *Chem. Soc. Rev.*, 2016, **45**, 3935–3953.

21   S. Bai, C. Pappas, S. Debnath, P. W. J. M. Frederix, J. Leckie, S. Fleming and R. V. Ulijn, *ACS Nano*, 2014, **8**, 7005–7013.

22   S. Fleming and R. V. Ulijn, *Chem. Soc. Rev.*, 2014, **43**, 8150–8177.

23   A. Lampel, R. V. Ulijn and T. Tuttle, *Chem. Soc. Rev.*, 2018, **47**, 3737–3758.

24   A. Baral, S. Roy, A. Dehsorkhi, I. W. Hamley, S. Mohapatra, S. Ghosh and A. Banerjee, *Langmuir*, 2014, **30**, 929–936.

25   T. O. Mason, T. C. T. Michaels, A. Levin, C. M. Dobson, E. Gazit, T. P. J. Knowles and A. K. Buell, *J. Am. Chem. Soc.*, 2017, **139**, 16134–16142.

26   M. Conejero-Muriel, J. A. Gavira, E. Pineda-Molina, A. Belsom, M. Bradley, M. Moral, J. de D. G.-L. Durán, A. Luque González, J. J. Díaz-Mochón, R. Contreras-Montoya, Á. Martínez-Peragón, J. M. Cuerva and L. Álvarez de Cienfuegos, *Chem. Commun.*, 2015, **51**, 3862–3865.

27   P. W. J. M. Frederix, G. G. Scott, Y. M. Abul-Haija, D. Kalafatovic, C. G. Pappas, N. Javid, N. T. Hunt, R. V. Ulijn and T. Tuttle, *Nat. Chem.*, 2015, **7**, 30–37.

28   J. K. Gupta, D. J. Adams and N. G. Berry, *Chem. Sci.*, 2016, **7**, 4713–4719.

29   X. Zhao, L. Xu, M. Sun, W. Ma, X. Wu, C. Xu and H. Kuang, *Nat. Commun.*, 2017, **8**, 2007.

30   B. S. Gomes, B. Simões and P. M. Mendes, *Nat. Rev. Chem.*, 2018, **2**, 0120.

31   J. J. Giner-Casares, G. Brezesinski and H. Möhwald, *Curr. Opin. Colloid Interface Sci.*, 2014, **19**, 176–182.

32   J. P. Coelho, M. J. Mayoral, L. Camacho, M. T. Martín-Romero, G. Tardajos, I. López-Montero, E. Sanz, D. Ávila-Brande, J. J. Giner-Casares, G. Fernández and A. Guerrero-Martínez, *J. Am. Chem. Soc.*, 2017, **139**, 1120–1128.

33   I. R. Sasselli, C. G. Pappas, E. Matthews, T. Wang, N. T. Hunt, R. V. Ulijn and T. Tuttle, *Soft Matter*, 2016, **12**, 8307–8315.

34   T. Li, M. Kalloudis, A. Z. Cardoso, D. J. Adams and P. S. Clegg, *Langmuir*, 2014, **30**, 13854–13860.

35   D. J. Adams, L. M. Mullen, M. Berta, L. Chen and W. J. Frith, *Soft Matter*, 2010, **6**, 1971-1980.

36   www.chemicalize.com (Accessed 12/09/2018)

ARTICLE

Journal Name

37   V. N. Viswanadhan, A. K. Ghose, G. R. Revankar and R. K. Robins, *J. Chem. Inf. Comput. Sci.*, 1989, **29**, 163–172.

38   G. Klopman, J.-Y. Li, S. Wang and M. Dimayuga, *J. Chem. Inf. Comput. Sci.*, 1994, **34**, 752–781.

39   T. J. Hou, K. Xia, W. Zhang and X. J. Xu, *J. Chem. Inf. Comput. Sci.*, 2004, **44**, 266–275.

40   M. Li, E. Zellermann and C. Schmuck, *Chem. Eur. J.*, 2018, **24**, 9061–9065.

41   N. Brown, J. Lei, C. Zhan, L. J. W. Shimon, L. Adler-Abramovich, G. Wei and E. Gazit, *ACS Nano*, 2018, **12**, 3253–3262.

42   E. R. Draper, H. Su, C. Brasnett, R. J. Poole, S. Rogers, H. Cui, A. Seddon and D. J. Adams, *Angew. Chem. Int. Ed.*, 2017, **129**, 10603–10606.

43   X. Mu, K. M. Eckes, M. M. Nguyen, L. J. Suggs and P. Ren, *Biomacromolecules*, 2012, **13**, 3562–3571.

44   S.-T. Wang, Y. Lin, R. K. Spencer, M. R. Thomas, A. I. Nguyen, N. Amdursky, E. T. Pashuck, S. C. Skaalure, C. Y. Song, P. A. Parmar, R. M. Morgan, P. Ercius, S. Aloni, R. N. Zuckermann and M. M. Stevens, *ACS Nano*, 2017, **11**, 8579–8589.

45   R. Contreras-Montoya, A. B. Bonhome-Espinosa, A. Orte, D. Miguel, J. M. Delgado-López, J. D. G. Duran, J. M. Cuerva, M. T. Lopez-Lopez and L. Álvarez de Cienfuegos, *Mater. Chem. Front.*, 2018, **2**, 686–699.

46   B. Adhikari, J. Nanda and A. Banerjee, *Soft Matter*, 2011, **7**, 8913-8922.

47   C. Rubia-Payá, G. De Miguel, M. T. Martín-Romero, J. J. Giner-Casares and L. Camacho, *Adv. Colloid Interface Sci.*, 2015, **225**, 134-145.

48   B. Adhikari and A. Banerjee, *Soft Matter*, 2011, **7**, 9259-9266.

49   Y. Zhou, P. F. Damasceno, B. S. Somashekar, M. Engel, F. Tian, J. Zhu, R. Huang, K. Johnson, C. McIntyre, K. Sun, M. Yang, P. F. Green, A. Ramamoorthy, S. C. Glotzer and N. A. Kotov, *Nat. Commun.*, 2018, **9**, 181.

50   H.-E. Lee, H.-Y. Ahn, J. Mun, Y. Y. Lee, M. Kim, N. H. Cho, K. Chang, W. S. Kim, J. Rho and K. T. Nam, *Nature*, 2018, **556**, 360–365.

51   V. P. Terrier, H. Adihou, M. Arnould, A. F. Delmas and V. Aucagne, *Chem. Sci.*, 2016, **7**, 339–345.

52   S. G. Booth, A. Uehara, S.-Y. Chang, C. La Fontaine, T. Fujii, Y. Okamoto, T. Imai, S. L. M. Schroeder and R. A. W. Dryfe, *Chem. Sci.*, 2017, **8**, 7954–7962.

53   G. Bodelón, V. Montes-García, C. Costas, I. Pérez-Juste, J. Pérez-Juste, I. Pastoriza-Santos and L. M. Liz-Marzán, *ACS Nano*, 2017, **11**, 4631–4640.

54   S. Paterson, S. A. Thompson, J. Gracie, A. W. Wark and R. de la Rica, *Chem. Sci.*, 2016, **7**, 6232–6237.

55   J. K. Sahoo, N. M. S. Sirimuthu, A. Canning, M. Zelzer, D. Graham and R. V. Ulijn, *Chem. Commun.*, 2016, **52**, 4698–4701.

56   W. Nuansing, A. Rebollo, J. M. Mercero, J. Zuñiga and A. M. Bittner, *J. Raman Spectrosc.*, 2012, **43**, 1397–1406.